A&A 520, A47 (2010)
DOI: 10.1051/0004-6361/201014331

Astronomy & Astrophysics

The blazar content in the *Swift*-BAT hard X-ray sky⋆

A. Maselli[1], G. Cusumano[1], E. Massaro[2], V. La Parola[1], A. Segreto[1], and B. Sbarufatti[1]

[1] INAF, Istituto di Astrofisica Spaziale e Fisica Cosmica di Palermo, via U. La Malfa 153, 90146 Palermo, Italy
e-mail: maselli@ifc.inaf.it
[2] Dipartimento di Fisica, Università La Sapienza, Piazzale A. Moro 2, 00185 Roma, Italy

Received 26 February 2010 / Accepted 8 June 2010

ABSTRACT

Aims. We present the results from a study of the blazar content in the 15–150 keV map of the entire sky obtained analysing 39 months of data collected by the BAT telescope aboard the *Swift* satellite.
Methods. We performed a cross-correlation of the significance map, obtained with a dedicated highly efficient algorithm for data processing and image reconstruction of the BAT survey data, with the blazar population of the *Roma*-BZCAT. After corrections for source confusion and spurious detections, we found significance excesses higher than two standard deviations for 304 sources, and the corresponding fraction of expected spurious associations is ∼20%. We selected hard X-ray blazars according to their significance level and carried out a statistical analysis to characterise their emission properties.
Results. A sample of 121 blazars detected at a significance level $\sigma > 3$ is discussed in greater detail. The fraction of blazars with uncertain classification in this sample is considerable (∼23%), more than twice the percentage obtained considering all the blazars classified in the *Roma*-BZCAT (∼9%). We attribute the X-ray flux of the majority of selected BL Lac objects to the synchrotron emission.

Key words. galaxies: active – BL Lacertae objects: general – radiation mechanisms: non-thermal

1. Introduction

Blazars constitute a peculiar class of radio-loud active galactic nuclei (AGNs) characterised by a strong non thermal emission over the whole electromagnetic spectrum. They show high and rapid variability and strong polarisation. In the radio band they appear as core-dominated, flat spectrum sources and the discovery of emission in the GeV (Abdo et al. 2009a) and TeV (see Weekes 2008, for a recent review) bands from an increasing number of these objects establishes them as a class of extreme particle accelerators. Within the framework of the AGN Unification Scenario (Urry & Padovani 1995), these properties are interpreted as non thermal radiation emitted by small size regions moving away from the central supermassive black hole at velocities close to the speed of light and at small angles with respect to the line of sight (Blandford & Rees 1978). This radiation is relativistically boosted and dominates all other components.

The spectral energy distributions (SED) of blazars are characterised by two distinct components in a Log $\nu F(\nu)$ vs. Log ν plot: the first one peaks at energies from IR to the X-ray band and the other one in the MeV-TeV range. According to the most widely adopted synchrotron self-Compton (SSC) scenario (Ghisellini & Maraschi 1989), the first SED component is caused by synchrotron radiation. These synchrotron photons, upscattered by the same population of electrons that generated them, would produce the second SED component by the inverse Compton process.

The blazar class includes BL Lac objects (BL) and flat spectrum radio quasars (FSRQs), which share the same overall shape in the SED but differ in the optical spectrum. BL objects display no or very weak emission lines, while FSRQs reveal evidence of broad emission lines. The *Roma*-BZCAT Catalogue (Massaro et al. 2009) provides one of the most complete lists of blazars based on data from literature and the April 2009 version includes 2837 objects. Sources are divided into three main types: 1006 BL Lac objects (BZB), 1577 flat spectrum radio quasars (BZQ), and 254 blazars with uncertain classification (BZU). This last class includes sources that exhibit some typical features of blazars, but with some ambiguities due either to a poor amount of data or to their transitional properties between FSRQs, BL Lacs, and other types of AGNs. Considering that the deepest surveys for blazar search were performed in the northern hemisphere, the sources listed in the *Roma*-BZCAT are characterised by a strong north-south asymmetry, with 1814 (64%) in the north and 1023 (36%) in the south sky.

Most blazars were initially selected in flux limited surveys in the radio and in the soft X-ray energy bands. Until recently, the study of their hard X-ray emission ($E > 10$ keV) has been hampered by difficulties in the imaging of sources with an adequate resolution through grazing incidence telescopes. A different technique is needed to obtain images of the hard X-ray sky, and significant results have been achieved with the coded mask aperture technique. At present, the Burst Alert Telescope (BAT, Barthelmy et al. 2005) aboard the *Swift* satellite (Gehrels et al. 2004) is performing the most sensitive and complete survey of the sky in the hard X rays. The analysis of progressively longer periods provided with BAT survey data has produced in recent years catalogues and lists of Galactic and extragalactic sources (Markwardt et al. 2005; Ajello et al. 2008; Tueller et al. 2008; Ajello et al. 2009b; Tueller et al. 2010). The largest (to date) hard X-ray catalogue, obtained from the reduction of 39 months of BAT survey data accumulated since its

⋆ Table 2 is only available in electronic form at the CDS via anonymous ftp to cdsarc.u-strasbg.fr (130.79.128.5) or via http://cdsarc.u-strasbg.fr/viz-bin/qcat?J/A+A/520/A47

launch, is the First Palermo BAT Catalogue (hereafter PBC39, Cusumano et al. 2010). It includes 754 identified objects of galactic and extragalactic nature detected with a high statistical significance; among extragalactic sources, 71 were classified as blazars.

We aimed at extending the information on blazar's hard X-ray emission to fainter sources than those identified in the PBC39. For this reason we cross-correlated the *Roma*-BZCAT Catalogue with the 39-month all-sky mosaic in the 15–150 keV energy band and found statistical evidence of emission in this range from a considerable fraction of the whole blazar population. The paper is organised as follows. In Sect. 2 we give some details about the BAT 39-month hard X-ray all-sky mosaic and in Sect. 3 we discuss the problem of confusion with bright non blazar objects. We characterise the blazar content of the BAT sky in Sect. 4 and describe its statistical properties in Sect. 5. In the last section we summarise our results.

2. The hard X-ray all-sky mosaic

For the analysis presented in this paper we used the 15–150 keV all-sky mosaic, obtained when processing the first 39 months of BAT survey with a code developed by some of us suitable for the analysis of data from coded mask telescopes. A detailed description of this code is reported in Segreto et al. (2010).

Our analysis is based on an all-sky map defined on a spherical grid, with a total number of 2.9×10^7 pixels corresponding to a spatial resolution of ~2.3 arcmin. A value of the significance σ, defined as the ratio between the intensity of the signal in the corresponding direction of the sky and the associated statistical error, is provided for each pixel.

The distribution of σ values of pixels in sky regions far from the sources is expected to be described by a Gaussian with zero mean and unitary standard deviation. However, an imperfect modelling of the instrumental properties introduces a number of systematic effects that may result in deviations from this Gaussian distribution and hence in false source detections and in a wrong evaluation of the source's significance. For this reason the actual S/N mean values and standard deviations were computed on a set of circular regions of radius 2.3 degrees, sampling the entire all-sky mosaic. These values were then interpolated to obtain the all-sky distribution of local mean values and standard deviations that was used to correct the mosaic intensity skymap and the associated statistical errors. Figure 1 shows the S/N distribution of all-sky mosaic pixels after the normalisation: excluding the positive tail due to the unsubtracted sources, this distribution is described very well by a Gaussian with zero mean and unitary standard deviation, as expected.

3. The problem of confusion with bright hard X-ray sources

The search for positional correlations between the 39-month all-sky significance map and the blazars included in the *Roma*-BZCAT Catalogue can be positively biased by the presence of bright hard X-ray sources. Figure 2 shows, as an example, the image of the sky region around the very bright low-mass X-ray binary EXO 0748-676, a source that lies outside the Galactic plane ($b \simeq -20°$). The positions of four FSRQs are very close to this source: two of them in particular fall well inside the region of influence of the PSF tail of the binary system, and the significance values at their positions is clearly biased towards positive values. A preliminary screening to avoid spurious associations due to this effect is therefore necessary.

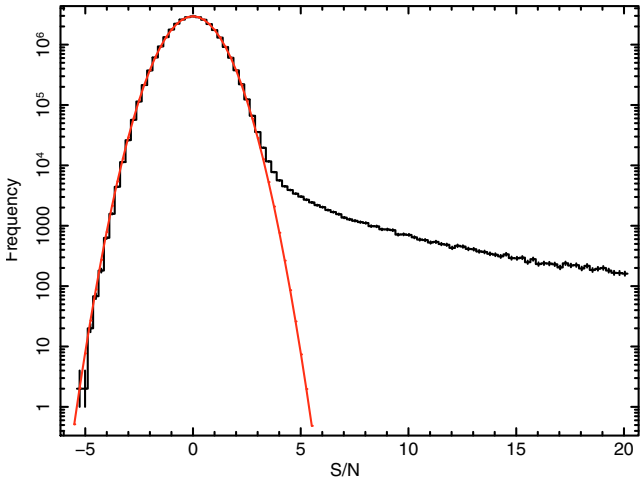

Fig. 1. The distribution of pixel significances in the BAT all-sky map corrected with locally measured means and standard deviations. The red line represents the Gaussian fit to the distribution, excluding its tail.

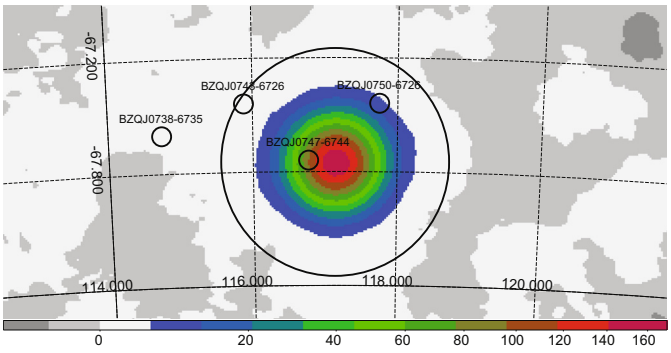

Fig. 2. A close-up of the BAT hard X-ray map centred on the low-mass X-ray binary EXO 0748-676. The grid coordinates are given in degrees. A circle with a radius $r = 36'$ marks the region of influence of bright sources in the map.

We adopted the conservative criterion of removing from the initial dataset of BZCAT blazars all sources close enough to the ~700 non-blazar objects included in the PBC39 ($\sigma > 4.8$). To estimate the size of the "radius of avoidance", we performed a test modifying the positions corresponding to all the PBC39 sources. We shifted them by increasing offset angles with steps of 0.1 deg until the distribution of the corresponding significances was consistent with a Gaussian law with $\mu = 0$ and $\sigma = 1$. This occurred for a value of the step corresponding to an offset angle of 36 arcmin, that is ~2 times the PSF of the instrument. A circle with this radius has been plotted in Fig. 2. We also verified that such radius is compatible with the region of influence of Cyg X-1 and Crab, the two brightest sources detected in the PBC39. The BZCAT blazars that fall within circular regions with $r = 36'$ centred on the PBC39 sources were therefore removed from the initial dataset for the subsequent analysis.

4. Blazars in the BAT sky

We used the screened list of 2762 *Roma*-BZCAT blazars to extract the corresponding values of the significance and built the related distribution. We only considered the σ value of the pixel associated with the source's coordinates, given with the precision

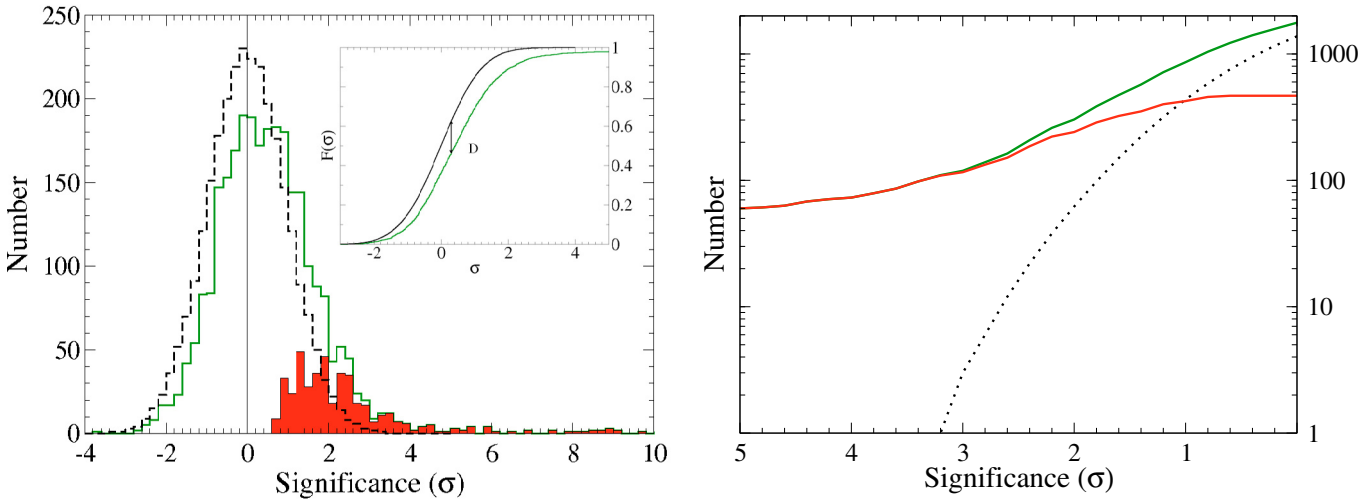

Fig. 3. *Left panel*: the histogram of the significance of the hard X-ray skymap at the positions of 2762 blazars included in the BZCAT (green solid line) and the mean histogram at the positions obtained scrambling their Galactic coordinates (black dashed line). The comparison between the corresponding cumulative distribution functions is plotted in the inset. The red filled histogram represents an estimate of the actual blazar contribution. *Right panel*: the number of associations with a significance higher than a specified value σ_T for the list of BZCAT blazars (green line) and for the net blazar contribution (red line). The black dotted line gives the number of spurious associations as a function of σ_T.

typical of radio or optical identification. The histogram in the left panel of Fig. 3 shows a very significant asymmetry with respect to the zero value expected for a random distribution: positive associations (1767) are nearly twice the negative ones (995). Excluding the sources above 5σ, the mean value and the standard deviation of the distribution are $\mu_{BZ} = 0.45 \pm 0.02$ and $\sigma_{BZ} = 1.16$, respectively. The large excess of positive σ values, reflecting in a significant deviation of μ_{BZ} from zero, is a strong indication of blazar's emission in the 15–150 keV hard X-ray range.

We repeated the same analysis using 20 lists of fictitious sources obtained by modifying the blazar's coordinates. To preserve the Galactic coordinate's distribution we scrambled the arrays of blazar Galactic latitudes and longitudes and extracted couples from these scrambled arrays. We removed from the datasets of modified coordinates the positions within 36′ from all the PBC39 sources and extracted the related distributions of σ values. We also built the mean distribution of these lists, which shows a substantial balance between positive and negative σ values. The corresponding histogram is plotted in the left panel of Fig. 3 and is characterised by 56 associations with $\sigma > 2$ and 3 associations with $\sigma > 3$. The difference between this mean distribution and the blazar distribution of σ values was verified applying a Kolmogorov-Smirnov test. The maximum difference D between the two cumulative distribution functions (inset of the left panel of Fig. 3) is $D = 0.18$, corresponding to a very low probability ($p < 2.2 \times 10^{-16}$) that they may be extracted from the same distribution. The parameters of a Gaussian fit to this mean distribution are consistent with $\mu = 0$ and $\sigma = 1$. Therefore we confidently used a distribution corresponding to a Gaussian law with $\mu = 0$ and $\sigma = 1$, normalised at the number of 2762 BZCAT blazars, to estimate the contribution of spurious associations. The net blazar content was then evaluated by subtracting the distribution corresponding to random associations to the blazar distribution. The result is shown in the left panel of Fig. 3 and includes 467 objects down to the lowest significance. It represents an estimate of the maximum number of cross-correlations between the currently available BAT map in the hard X rays and the BZCAT catalogue.

The number of associations with a significance higher than a specified threshold value σ_T is plotted in the right panel of Fig. 3 for the distributions of the BZCAT blazars and of the net blazar content, together with the number of expected spurious associations. The estimated numbers of spurious associations (62 for $\sigma_T = 2$ and 3 for $\sigma_T = 3$) agree with the results obtained by the mean distribution of pseudo-random positions. The fraction of expected spurious associations at a determined σ_T value can be derived from the curves in Fig. 3 (right panel). The probability that a given fraction of the sample collected at $\sigma > \sigma_T$ is made of spurious sources can then be obtained by applying the results of the binomial distribution. We calculated the probability that at least 50% of the sample is spurious, and we found it negligible for both $\sigma_T = 2$ ($p \simeq 10^{-30}$) and $\sigma_T = 3$ ($p \simeq 10^{-61}$). The blazars detected at $\sigma > 4.8$ are 61, less than those (71) included in the PBC39. The origin of this discrepancy is that PBC39 reported the results of a combined analysis on three energy bands (15–30 keV, 15–70 keV, and 15–150 keV), while our analysis was carried out only on the 15–150 keV map. Then, a few blazars included in the PBC39 have been detected at a sigma level higher than 4.8 only in the 15–30 and 15–70 keV maps. Assuming that this sample of 61 blazars above $\sigma_T = 4.8$ is complete (e.g. accurate identifications, no spurious sources) and that it has a standard Log N-Log S

$$N(>S) = KS^{-\alpha} \quad (1)$$

with $\alpha = 1.5$, we should expect to find 123 and 227 blazars above $\sigma_T = 3$ and $\sigma_T = 2$, respectively. Our results (118 blazars for $\sigma_T > 3$ and 242 for $\sigma_T > 2$, right panel of Fig. 3) are in acceptable agreement with these estimates.

5. Properties of blazars associated with positive signals

We investigated the general properties of the blazars associated with positive values of the significance, making a distinction in the blazar type (BZB, BZQ, and BZU sources) according to the classification reported in the BZCAT. Moreover, we

Table 1. The results of the statistical analysis on different blazars types detected in our BAT hard X-ray map.

BZ type	σ_T	Number (%)	$\langle z \rangle$	$\langle f_r \rangle^{(1)}$	$\langle F_{SX} \rangle^{(2)}$	$\langle F_{HX} \rangle^{(2)}$
BZB		1006 (35.5)	0.17	156	2.5	
	4.8	14 (23.0)	0.16	1089	30.1	28.8
	3	24 (19.8)	0.14	708	21.3	19.6
	2	71 (23.3)	0.18	406	14.2	9.8
BZQ		1577 (55.5)	1.41	592	0.4	
	4.8	31 (50.8)	1.38	4630	4.4	33.9
	3	69 (57.0)	1.24	2799	2.7	19.4
	2	185 (60.9)	1.23	1508	1.4	10.4
BZU		254 (9.0)	0.40	923	1.8	
	4.8	16 (26.2)	0.16	4743	18.0	93.7
	3	28 (23.2)	0.17	3953	11.1	56.8
	2	48 (15.8)	0.22	2520	7.0	35.2

Notes. [(1)] The radio flux density f_r is given in mJy; [(2)] the soft X-ray flux F_{SX} and the hard X-ray flux F_{HX} are given in 10^{-12} erg cm^{-2} s^{-1}.

considered the further classification of BL Lac sources into low-energy (LBL) and high-energy (HBL) peaked BL Lac objects (Padovani & Giommi 1995). This classification was adopted to take the range of variation of their synchrotron peak frequency ν_p into account: LBLs peak mainly in the infrared-optical range, while HBLs do in the UV-X ray domain. FSRQs do not share the same behaviour and their SEDs are similar to those of LBL sources. The ratio between the X-ray and the radio emission has proved to be a reliable index for classification of BL Lac objects as LBL or HBL (Giommi et al. 1999). We expressed this ratio adopting a convenient adimensional factor (Maselli et al. 2010)

$$\Phi_{XR} = 10^{-3} \cdot \frac{F_{SX}}{S_{1.4}\,\Delta\nu} \tag{2}$$

where F_{SX} is the flux in the soft (0.1–2.4 keV) X-ray band, $S_{1.4}$ is the radio flux density at 1.4 GHz and $\Delta\nu = 1$ GHz. With the scale factor 10^{-3}, the value of $F_{SX}/S_{1.4} = 10^{-11}$ erg cm^{-2} s^{-1} Jy^{-1} corresponds to $\Phi_{XR} = 1$, which can be considered a lower limit for HBL sources (Maselli et al. 2009).

We selected the lists of the three main blazar types and carried out a statistical analysis of some physical quantities reported in the BZCAT (Massaro et al. 2009): the redshift, the radio flux density S at 1.4 GHz, and the X-ray flux F_{SX} in the soft band (0.1–2.4 keV). Only firm estimates of the redshift were considered: 79 (7.9%) BZB, 20 (1.3%) BZQ, and 29 BZU (11.4%) sources were then excluded in the calculation of the mean redshift values. The optical magnitude was not considered because possibly affected by the host galaxy emission for the near sources. To these elements we added the X-ray flux F_{HX} in the hard band (15–150 keV) obtained from the conversion of the source's count rate that we measured from the BAT survey data. The conversion factor was derived using the corresponding count rate and the Crab spectrum used for BAT calibration purposes, as explained in the BAT calibration status report[1]. For each blazar type, the analysis was carried out both over the whole population of sources classified in the BZCAT and over a selection of hard X-ray blazars detected at a significance level higher than a threshold σ_T. We reported in Table 1 the results obtained assuming three different σ_T values. The expected contamination for spurious association increases from 2.5% at $\sigma_T = 3$ to 20.4% at $\sigma_T = 2$, and exceeds 50% for $\sigma_T < 1.0$. The numbers of sources reported in the third column of Table 1, and the corresponding percentages, refer to the blazar subsample as a whole or to a selection of hard X-ray blazars. These percentages change differently for the three blazar types when the number of faint sources (i.e. for decreasing σ_T) increases. Among the sources selected at $\sigma > 4.8$ a considerable percentage (~26%) of blazars with uncertain classification is found. This decreases to ~16% by including sources down to $\sigma = 2$, while the corresponding number of FSRQs increases from ~51% up to ~61%. The variations in the significance threshold do not affect the fraction of BLs in any considerable way.

The reduction of the significance threshold follows in the simultaneous decrease of the mean radio and X-ray fluxes of the three blazar classes. This result indicates that sources with lower σ values are intrinsically fainter and are characterised by lower fluxes in all the considered energy bands. The mean redshift of blazars with uncertain classification ($\langle z \rangle = 0.40$) is nearly twice with respect to BL Lac object's ($\langle z \rangle = 0.17$); the values obtained considering the sources detected in the hard X rays are instead very similar for BZBs and BZUs at the three considered σ_T values. Both types of sources are considerably closer to the observer than flat spectrum radio quasars (BZQ), whose mean redshift value is higher than $z = 1$. The comparison between the mean redshift values that we obtained and those reported by Ajello et al. (2009b) leads to similar results. Considering blazars selected at $\sigma > 4.8$, we found $z_B = 0.16$ for BZB sources and $z_Q = 1.38$ for BZQ sources; Ajello et al. (2009b) quote $z_B = 0.11$ and $z_Q = 1.63$, respectively.

The results reported in Table 1 point out that a considerable fraction of BL Lac sources are of the HBL type, for which the flux in the radio band is lower than FSRQ's, and the synchrotron component is shifted towards high frequencies, peaking in the X-ray domain. In contrast, the X-ray emission of FSRQs, as well as that of LBLs, is due to the inverse Compton component that has a harder spectrum and expected peaks in the γ-ray band (Abdo et al. 2009a). The BZU blazars are confirmed as "out of scheme" sources and are characterised by peculiar features. The mean values of their fluxes are very high at all the considered frequencies; in particular, in the radio band their flux densities are approximately six times higher than BL Lac object's. The mean value of their hard X-ray flux is five times higher than the one in the soft band following in a hard X-ray spectrum, similar to FSRQ's. The analysis of their spectral energy distribution confirms their peculiarity: in a large number of cases it is quite difficult to distinguish well-defined synchrotron and inverse Compton emission components. For this reason they set aside in the general picture mentioned above for FSRQs and BL Lac Objects.

We examined the distribution of the X-ray fluxes, both in the soft (0.1–2.4 keV) and in the hard (15–150 keV) bands, of sources detected at a significance level $\sigma > 2$. In Fig. 4 we distinguished the blazar type by adopting different symbols and colours. A large number of sources are found in a region with typical values of F_{HX} around 5×10^{-12} erg cm^{-2} s^{-1}, with a broad span in the soft X-ray flux F_{SX} of more than three decades. We traced a line in the plot that marks a balance between F_{SX} and F_{HX}: in the region I the hard X-ray flux is in excess with respect to the soft one, and vice versa. We found that the region II is mainly populated by BL Lac objects, while FSRQs are only located in the region I of the plot. We identified the BL Lac sources that are found in the region I, at high separation from the line. These are well-known sources, with a synchrotron peak frequency far from the X-ray band and generally classified as LBL objects. Among them we point out BL Lac, which is one of the very few LBL objects with a detection in

[1] http://swift.gsfc.nasa.gov/docs/swift/analysis/bat_digest.html

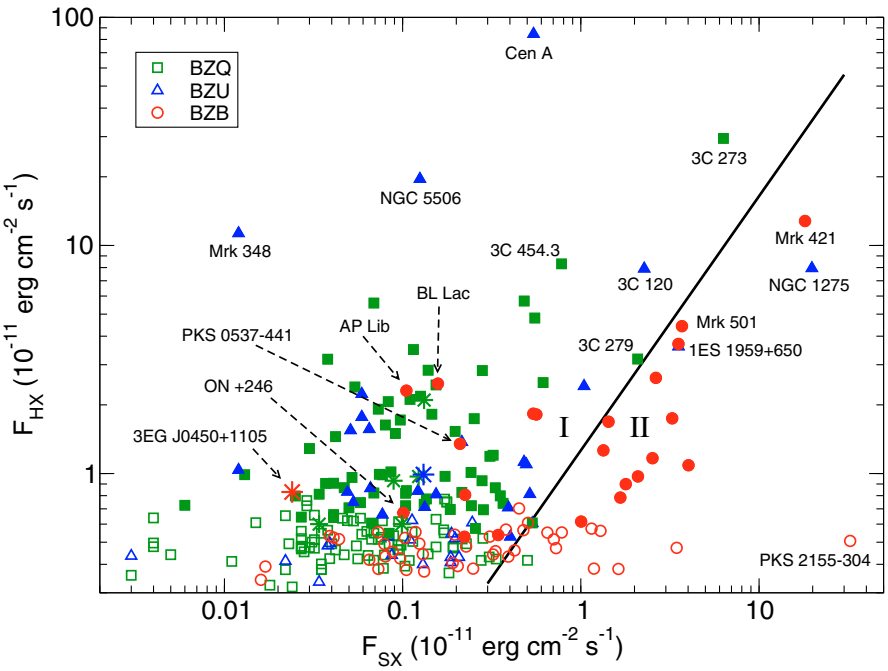

Fig. 4. The X-ray fluxes in the soft (0.1–2.4 keV) and in the hard (15–150 keV) X-ray bands for the blazars detected at $\sigma > 2$. Red circles, green squares, and blue triangles have been used for BZB, BZQ, and BZU sources, respectively. Filled symbols distinguish sources with $\sigma > 3$. Sources with a soft X-ray flux derived by recent *Swift*-XRT observations are marked by a star. The line marks a region of balance between F_{SX} and F_{HX}.

the TeV range (Abdo et al. 2009b). Like the majority of FSRQs, their hard X-ray spectra belong to the Compton component. For these sources $\Phi_{XR} \ll 1$, as reported in Table 2. In contrast, the large majority of BZB sources populating region II is of the HBL type: in Fig. 4 we indicated those that are most known. In particular, we point out PKS 2155-304, an intense source characterised by a very soft X-ray spectrum, and Mrk 421, which in recent years went through a phase of very intense activity (Tramacere et al. 2009) characterised by the hardening of the X-ray flux. A fraction of HBL sources can be more easily found in region I by adopting lower significance values, down to $\sigma_T = 1$: however, we attribute this effect to the large number of spurious associations that correspond to such a low significance threshold. Another comment is appropriate for NGC 1275. This BZU source is hosted in a giant elliptical galaxy lying at the centre of the Perseus cluster. The spectral analysis carried out by Ajello et al. (2009a) on *Swift*-XRT and *XMM-Newton* observations points out a hard X-ray spectrum with a photon index $\Gamma = 1.6$. According to the values used in our analysis, the flux in the hard X-ray band is nearly half of the one in the soft band. The possibility that, in this case, the value of the soft X-ray flux adopted by us may include a relevant contribution of thermal origin from the Perseus cluster cannot be rejected.

We report in Table 2 the list of hard X-ray blazars obtained when adopting $\sigma_T = 3$ as the detection threshold: with this choice a number of three spurious sources over a total of 121 blazars (~2.5%) is expected. We obtained 69 FSRQs, 24 BL Lac objects, and 28 blazars of uncertain classification, representing 4.4%, 2.4%, and 11.0% of the corresponding populations classified in the BZCAT, respectively. Notably, among the top 10 sources there are five BZU such as Centaurus A (the brightest blazar detected), followed by NGC 5506, Mrk 348, NGC 1275, and 3C 120. For each blazar we report in Table 2 the BZCAT name (Col. 1), an alternative name (Col. 2), the coordinates (Cols. 3, 4), and the redshift (Col. 5; uncertain estimates are given with a question mark); the flux in the soft X-ray band (Col. 6), the Φ_{XR} values (Col. 7) and the significance in the 39-month BAT 15-150 all-sky map (Col. 8). We also report whether the blazar is included in other lists and catalogues such as the 22-month catalogue by Tueller et al. (2010, Col. 9), the blazar sample collected by Ajello et al. (2009b, Col. 10), and the PBC39 (Cusumano et al. 2010, Col. 11). The analysis of Tueller et al. (2010) is based on a survey in the 14–195 keV band, while Ajello et al. (2009b) restricted their analysis to the 15–55 keV energy interval. Moreover, Ajello et al. (2009b) limited their analysis to BL Lacs and FSRQs; the only BZU object included in their list comes from a different classification with respect to BZCAT. A few sources that lack a detection in the RASS (Voges et al. 1999) and observations by other telescopes have been recently observed by the XRT telescope aboard *Swift*. Their fluxes were calculated in the 0.5–2.0 keV band following the same procedure as adopted in Massaro et al. (2009). We report their fluxes with an asterisk in Table 2 and we mark them in Fig. 4. Only one source (BZQJ0432-5109) lacks a detection in the soft X-ray band.

The comparison of this sample with the one collected by Ajello et al. (2009b) shows that, after excluding five objects (4C 29.06, RBS 315, IGR J03532-6829, B2 1210+33, S5 2116+81) not included in the BZCAT, all the remaining 33 sources are present in our sample. The main fraction of FSRQs vs. BL Lacs (68.4% and 31.6%, respectively) reported by them is practically identical to the one obtained by us (68.9% vs. 31.1%). The percentages only moderately change lowering the significance threshold: we found 74.2% and 25.8% for $\sigma_T = 3$, while 72.3% and 27.7% are obtained for $\sigma_T = 2$.

We found an estimate of the peak frequency ν_p of the synchrotron emission in Nieppola et al. (2006) for half of the BL Lac objects, observable from the northern emisphere. The large majority of them are classified as HBLs with ν_p values spanning a range from $\nu_p = 16.49$ (PG 1553+113) to $\nu_p = 21.05$ (1H 0658+595). The Φ_{XR} values reported in Table 2, as well as the position of these sources in Fig. 4, agree with these estimates of the peak frequency and confirm the HBL nature of the large majority of the hard X-ray BL Lac objects, as already found by

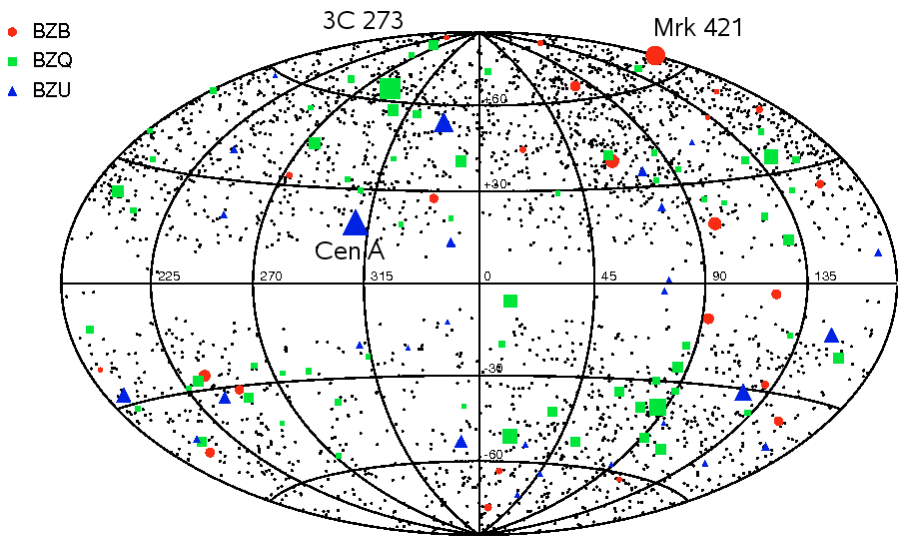

Fig. 5. The Aitoff projection in Galactic coordinates showing the distribution of all blazars classified in the BZCAT (black dots). The 121 sources detected in the BAT all-sky map at $\sigma > 3$ are plotted with different colours to distinguish 69 flat spectrum radio quasars, 24 BL Lacs, and 28 blazars of uncertain classification.

Ajello et al. (2009b). An exception is found in by BL Lac and ON +246, for which Nieppola et al. (2006) give an estimate of $\nu_p = 14.28$ and $\nu_p = 14.9$, respectively. Both sources are characterised by $\Phi_{XR} < 1$ and are found in the region I of the plot in Fig. 4, as expected for sources with a synchrotron peak frequency far from the X-ray range.

Figure 5 shows the position of the 121 selected objects among all *Roma*-BZCAT blazars in an Aitoff projection of the sky in Galactic coordinates. The size of the symbols is proportional to the significance of the detection, and the name of the sources with the highest significance for each blazar type has been reported. Only a few blazars at a very low Galactic latitude are included in the BZCAT, due to the corresponding lack of data in the main surveys. Still, a few associations with hard X-ray emitters has been found. We rejected the possibility of confusion with galactic sources after a SIMBAD query in a 5′ radius circle centred on their position. This value of the radius accounts for the BAT error circle of selected sources characterised by lower σ values.

6. Conclusions

Our analysis shows that an appreciable fraction of the sources listed in the BZCAT is associated to a positive value in the significance map of the BAT sky. This result was obtained using a statistical approach based on the differences between the distribution function corresponding to the blazar positions and other distributions obtained after modifications of blazar's coordinates. We estimated that 467 associations with BZCAT sources are likely genuine, while 242 of them have $\sigma > 2$. At lower significance values, the number of associations with positive fluctuations is, of course, even higher and reaches 350 sources in the interval $0.6 < \sigma < 3$, more than 12% of the blazars in the *Roma*-BZCAT. Fixing the detection threshold at $\sigma_T = 3$, we identified 121 blazars with respect to the 71 objects included in the First Palermo BAT Hard X-ray Catalogue (PBC39, Cusumano et al. 2010), with an increment of ~70%. This sample includes the 71 blazars reported in the PBC39 and the 33 objects in the list of Ajello et al. (2009b) included in the BZCAT. The corresponding fraction of expected spurious association is ~2.5%. Notably, 23% of our sample is made up of blazars with uncertain classification. The statistical analysis that we carried out on the different types of blazars characterises their emission properties. In particular, the distribution of sources in a F_{HX} vs. F_{SX} plot emphasises the separation of selected BL Lac objects from FSRQs, establishing the HBL classification for a high fraction of them. Possible departures from some of our results occur when sources with very low significance values, down to $\sigma = 1$, are included in the sample used for the statistical analysis: however, we consider that they are mainly due to the sizable fraction of spurious BAT-BZCAT associations.

Acknowledgements. The authors are grateful to the referee Marco Ajello for the suggestions that helped to substantially improve the paper. They acknowledge financial support by ASI/INAF through contract I/011/07/0. Part of this work is based on archival data, software or online services provided by the ASI Science Data Center (ASDC) and by the SIMBAD database, which is operated at the CDS, Strasbourg, France.

References

Abdo, A. A., Ackermann, M., Ajello, M., et al. 2009a, ApJ, 700, 597
Abdo, A. A., Ackermann, M., Ajello, M., et al. 2009b, ApJ, 707, 1310
Ajello, M., Greiner, J., Kanback, G., et al. 2008, ApJ, 678, 102
Ajello, M., Rebusco, P., Cappelluti, N., et al. 2009a, ApJ, 690, 367
Ajello, M., Costamante, L., Sambruna, R. M., et al. 2009b, ApJ, 699, 603
Barthelmy, S. D., Barbier, L. M., Cummings, J. R., et al. 2005, Space Sci. Rev., 120, 143
Blandford, R. D., & Rees, M. J. 1978, Proceedings of Pittsburgh Conference on BL Lac objects
Cusumano, G., La Parola, V., Segreto, A., et al. 2010, A&A, 510, A48
Gehrels, N., Chincarini, G., Giommi, P., et al. 2004, ApJ, 611, 1005
Ghisellini, G., & Maraschi, L. 1989, ApJ, 340, 181
Giommi, P., Menna, M. T., & Padovani, P. 1999, MNRAS, 310, 465
Górski, K. M., Hivon, E., Banday, A. J., et al. 2005, ApJ, 622, 759
Markwardt, C. B., Tueller, J., Skinner, G. K., et al. 2005, ApJ, 633, L77
Maselli, A. 2009, Ph.D. Thesis, Sapienza University of Rome
Maselli, A., Massaro, E., Nesci, R., et al. 2010, A&A, 512, A74
Massaro, E., Giommi, P., Leto, C., et al. 2009, A&A, 495, 691
Nieppola, E., Tornikoski, M., & Valtaoja, E. 2006, A&A, 445, 441
Padovani, P., & Giommi, P. 1995, ApJ, 444, 567
Segreto, A., Cusumano, G., Ferrigno, C., et al. 2010, A&A, 510, A47
Tramacere, A., Giommi, P., Perri, M., et al. 2009, A&A, 501, 879
Tueller, J., Mushotzky, R. F., Barthelmy, S., et al. 2008, ApJ, 681, 113
Tueller, J., Baumgartner, W. H., Markwardt, C. B., et al. 2010, ApJS, 186, 378
Urry, C. M., & Padovani, P. 1995, PASP, 107, 803
Voges, W., Aschenbach, B., Boller, T., et al. 1999, A&A, 349, 389
Weekes, T. C. 2008, High Energy Gamma-Ray Astronomy, ed. F. A. Aharonian, W. Hofmann, & F. Rieger (San Francisco, CA: ASP), AIP Conf. Ser., 1085